

TRADEOFF ANALYSIS OF OFFSHORE STRUCTURES UNDER STOCHASTIC EXCITATION

Hector A. Jensen, Danilo S. Kusanovic and Marcos A. Valdebenito

*Department of Civil Engineering, Santa Maria University, Av. España 1680, Valparaiso, Chile,
hector.jensen@usm.cl*

Keywords: Compromise programming, Multi-objective optimization, Stochastic simulation, Stochastic sea model, Reliability-based design.

Abstract.

The analysis and design of structural systems such as offshore structures usually involve several design goals which are required to be maximized or minimized simultaneously. The design goals are in general potentially conflicting requirements reflecting technical and economical performances. The purpose of this work is to obtain in an efficient manner compromise designs that best represent the outcome that the designer considers potentially satisfactory. The designs are obtained by formulating a compromise programming problem, which is solved by an efficient first-order interior point algorithm. In order to exemplify the proposed methodology a typical offshore structural model is considered for analysis. The random sea is modeled as a Gaussian process following a Joint North Sea Wave Observation Project (JONSWAP) type spectrum for free surface elevation. Numerical results show that the proposed approach for decision making is quite effective.

1 INTRODUCTION

The design and optimization of complex engineering problems such as offshore structures usually involve several design goals which are required to be maximized or minimized while satisfying a number of design constraints. These design goals are potentially conflicting requirements reflecting technical and economical performances of a given system design. To accommodate these conflicting design goals and to explore the design options, the optimization problem is formulated in terms of a multi-objective optimization procedure (Steuer, 1986). An important class of solutions to the multi-objective problem is said to belong to the Pareto front (set of Pareto optimal solutions). Each solution or alternative design comprising the front is understood to be Pareto optimal which means there are no other design alternatives for which all objectives are better (Stadler, 1992; Miettinen, 1999). The selection of one of the Pareto design alternative over another is a matter of decision-maker preference.

Classical methods for generating the Pareto optimal set combine the objectives into a single parameterized function. These methods involve assigning a weight to each objective function. Several optimization runs with different settings are performed in order to generate the Pareto optimal set. The results of the identification of a particular design depend on the set of weights used in the analysis. The single objective problem is computationally attractive since conventional minimization algorithms can be applied to solve the problem (Rao et al, 1988; Ulrich and Eppinger, 2000; Papadrakakis et al, 2002). The main limitation of weighted sum methods is that they do not yield solutions that lie in non-convex regions of the feasible design space. In practice this means that weighted sum methods could miss potentially preferable designs. Additional procedures available for the generation of compromise solutions with various capabilities and limitations, include goal programming, physical programming, interactive methods, and methods based on genetic algorithms (Messac and Mattson, 2002; Tappeta and Renaud, 1999; Goldberg, 1989; Papadimitriou, 2005). In general, the determination of the entire Pareto front is prohibitively expensive for complex structural systems. This is the case of dynamical systems under stochastic loading such as offshore structures subject to water wave excitation.

The aim of this work is restricted to obtain in an efficient manner compromise solutions that best represent the outcome that the designer considers potentially satisfactory. This type of information provides a useful tool for the designer or analyst for decision making and tradeoff analysis, since it allows an efficient design exploration around specific Pareto points. To exemplify the proposed methodology a typical offshore structural model is considered for analysis. The random sea is modeled as a Gaussian process following a Joint North Sea Wave Observation Project (JONSWAP) type spectrum for free surface elevation (Hasselmann and Olbers, 1973).

2 PROBLEM FORMULATION

Consider a multi-objective optimization problem defined as the identification of a vector $\{\chi\}$, $\chi_i, i = 1, \dots, n_d$, of design variables to minimize a vector of objective functions

$$\{c(\{\chi\})\} = \{c_1(\{\chi\}), c_2(\{\chi\}), \dots, c_{n_c}(\{\chi\})\} \quad (1)$$

subject to

$$g_j(\{\chi\}) \leq 0, \quad j = 1, \dots, n_g \quad (2)$$

$$\{\chi\} \in \Xi \quad (3)$$

where $c_i, i = 1, \dots, n_c$ are the objective functions, $g_j, j = 1, \dots, n_g$ are the constraints functions, and Ξ is the set that contains the side constraints for the vector of design variables. The objective and constraint functions can be defined in terms of initial costs, repair and replacement costs, downtime costs, reliability measures, etc. For structural systems under stochastic loading the reliability measures are usually defined in terms of failure probability functions. For a given design $\{\chi\}$ the failure probability function $P_F(\{\chi\})$ can be expressed in terms of the multidimensional probability integral

$$P_F(\{\chi\}) = \int_{\Omega_F(\{\chi\})} p(\{\theta\}) d\{\theta\} \quad (4)$$

where $\Omega_F(\{\chi\})$ is the failure domain corresponding to the failure event F evaluated at the design $\{\chi\}$, and $\{\theta\}, \theta_i, i = 1, \dots, n_u$ is the vector of uncertain system parameters involved in the problem, i.e. uncertain structural parameters and excitation. The uncertain system parameters are modeled using a prescribed probability density function $p(\{\theta\})$. This function indicates the relative plausibility of the possible values of the uncertain parameters $\{\theta\} \in \Omega_{\{\theta\}} \subset R^{n_u}$. For systems under stochastic excitation the probability that design conditions are satisfied within a particular reference period (first excursion probability) provides a useful reliability measure. In this case, the failure event $F(\{\chi\}, \{\theta\})$ is defined as

$$F(\{\chi\}, \{\theta\}) = \max_{i=1, \dots, n_s} \max_{t \in [0, t_s]} |s_i(t, \{\chi\}, \{\theta\})| \geq s_i^* \quad (5)$$

where $[0, t_s]$ is the time interval of analysis, $s_i(t, \{\chi\}, \{\theta\}), i = 1, \dots, n_s$ are the response functions associated with the failure criterion F , and s_i^* is the corresponding critical threshold level. The response functions $s_i(t, \{\chi\}, \{\theta\}), i = 1, \dots, n_s$ are obtained from the solution of the equation of motion that characterizes the structural model.

3 COMPROMISE PROGRAMMING

The determination of a set of non-dominated solutions (Pareto optimum solutions) of the above multi-objective optimization problem achieves a compromise among different objective functions. As previously pointed out there are a number of procedures available for the generation of compromise solutions with various capabilities and limitations. The objective of this work is to obtain in an efficient manner particular compromise solutions. To this end, the set of compromise solutions is defined by means of the so-called ideal point, $\{c^{(id)}\}, c_i^{id}, i = 1, \dots, n_c$, which contains the individual optima of each of the objective functions. The approach, which is called compromise programming (CP) is based on the minimization of the distance between the ideal point and the Pareto set (Steuer, 1986). In particular, the Tchebyshev norm (Sawaragi et al, 1985; Jensen, 2009) is used to measure such distance in the present implementation. The corresponding compromise programming problem to the multi-objective optimization problem (1-3) can be written as

$$\text{Min } z \quad (6)$$

subject to

$$z \geq \frac{c_i(\{\chi\}) - c_i^{id}}{c_i^{as} - c_i^{id}}, i = 1, \dots, n_c \quad (7)$$

$$g_j(\{\chi\}) \leq 0, j = 1, \dots, n_g \quad (8)$$

$$\{\chi\} \in \Xi, \quad z \geq 0 \quad (9)$$

where z is an auxiliary variable. The components $c_i^{\text{as}}, i = 1, \dots, n_c$ are called the aspiration levels and they are defined by the designer or analyst prior to solving the compromise programming problem. These aspiration levels represent the outcomes that the designer feels adequate, and they can only be achieved when they are on the compromise set. In other cases, a Pareto point that best represents the aspiration levels is obtained.

4 TRADEOFF ANALYSIS

The sensitivity analysis at a given Pareto solution provides the variation in one objective given the variation in another objective on the Pareto surface in a given direction. In particular, the sensitivity along the feasible descent direction of each of the objectives in the objective function space is considered here. Let $\{\chi^*\}$ be the design corresponding to the Pareto solution that best represents the designer aspiration level, and J the active constraint set defined as

$$J = \{j : g_j(\{\chi^*\}) = 0, j = 1, \dots, n_g\} \quad (10)$$

The feasible direction $\{dc_i\}$ with the greatest improvement of the objective c_i is obtained by projecting the gradient vector $-\nabla_{\chi} c_i(\{\chi^*\})$ onto the projection matrix $[P]$ of the active constraint set, that is,

$$\{dc_i\} = -[P] \nabla_{\chi} c_i(\{\chi^*\}) \quad (11)$$

where the projection matrix is given by

$$[P] = [I] - [B]^T([B][B]^T)^{-1}[B] \quad (12)$$

and where the rows of the matrix $[B]$ are the gradients of the active constraints (constraints in J and the active bounds) (Belegundu and Chandrupatla, 1999). The vector $\{dc_i\}$ corresponds to the projection of the steepest descent direction of the objective c_i onto the tangent plane defined by the active constraints at $\{\chi^*\}$. The Pareto sensitivity measure $\delta c_i / \delta c_j$, i.e., the variation in the objective function c_i given the variation in the objective function c_j , along the feasible descent direction of the objective c_j is given by the projection of $\{dc_i\}$ onto the direction $\{dc_j\}$, that is

$$\delta c_i / \delta c_j = \frac{\{dc_i\}^T \{dc_j\}}{\{dc_j\}^T \{dc_j\}} \quad (13)$$

This equation represents the tradeoff information of the objective c_i along the feasible descent direction of the objective c_j . The sensitivity information given by Eq. (13) requires the sensitivity evaluation of the quantities involved in the optimization problem (1-3). The evaluation of such sensitivities is discussed in a subsequent section.

5 NUMERICAL IMPLEMENTATION

5.1 Solution of compromise optimization problem

For solving the optimization problem posed in (6-9), a nonlinear interior point method is implemented here. Starting from an interior point the objective of the method is to determine a direction vector $\{v\}$ followed by a step length along this direction which gives a new improved design point (Haftka and Gürdal, 1992). In particular, a scheme that moves along the active

constraints to reach the solution point is used in the present implementation. In this algorithm the direction $\{v\}$ corresponds to a descent feasible direction and it is computed by solving a linear programming subproblem (Haftka and Gürdal, 1992). The characterization of the linear problems involves the gradients of the objective and constraint functions. Once a direction $\{v\}$ has been obtained, a one dimensional search is carried out (line search). The process continues until convergence is achieved.

5.2 Reliability estimation

It is noted that some of the quantities involved in the compromise optimization problem are given in terms of reliability measures which are characterized by failure probability functions. In order to compute these quantities a high-dimensional integral needs to be evaluated. This difficulty favors the application of Monte Carlo Simulation as fundamental approach to cope with the probability integrals. However, in most engineering applications the probability that a particular system fails is expected to be small, e.g. between $10^{-4} - 10^{-6}$. Direct Monte Carlo is robust to the type and dimension of the problem, but it is not suitable for finding small probabilities. Therefore, advanced Monte Carlo strategies are needed to reduce the computational efforts. In particular a generally applicable method, called subset simulation, is implemented in this work (Au and Beck, 2001).

5.3 Sensitivity estimation

The proposed solution strategy requires the gradients of the functions associated with the compromise optimization problem in order to identify search directions. In particular, the estimation of the sensitivity of the constraints involving probability terms can be a challenging task. Thus, a specialized approach for estimating the sensitivity of these quantities is considered here. The approach is based on the approximate representation of two different quantities. The first approximation involves the demand function while the second includes the failure probability function. The failure domain Ω_F for a given design $\{\chi\}$ can be defined as

$$\Omega_F(\{\chi\}) = \{\{\theta\} \mid \kappa(\{\chi\}, \{\theta\}) \geq 1\}. \quad (14)$$

where κ is the demand function. If $\{\chi^k\}$ is the current design, the demand function κ is approximated in the vicinity of the current design as

$$\bar{\kappa}(\{\chi\}, \{\theta\}) = \kappa(\{\chi^k\}, \{\theta\}) + \{\delta\kappa\}^T \{\Delta\chi\} \quad (15)$$

where $\{\chi\} = \{\chi^k\} + \{\Delta\chi\}$. For samples $(\{\theta_i\})$, $i = 1, \dots, M$ near the limit state surface, that is, $\kappa(\{\chi\}, \{\theta_i\}) \approx 1$, the demand function is evaluated at points in the neighborhood of $\{\chi^k\}$, and the coefficients $\{\delta\kappa\}$ of the approximation are computed by least squares. Since the samples $(\{\theta_i\})$, $i = 1, \dots, M$ are chosen near the limit state surface the approximate demand function $\bar{\kappa}$ is expected to be representative, on the average, of the behavior of the failure domain Ω_F in the vicinity of the current design $\{\chi^k\}$ (Valdebenito and Schuëller, 2009). Next, the failure probability function, evaluated at the current design $\{\chi^k\}$, is approximated locally as an explicit function of the normalized demand around $k^* = 1$ as

$$P[\kappa(\{\chi^k\}, \{\theta\}) \geq \kappa^*] \approx e^{\psi_0 + \psi_1(\kappa^* - 1)}, \quad (16)$$

$$\kappa^* \in [1 - \epsilon, 1 + \epsilon]$$

where κ^* is a threshold of the normalized demand (in the neighborhood of one) and ϵ represents a small tolerance. The coefficients ψ_0 and ψ_1 can be calculated by least squares with samples of the demand function κ generated at the last stage of subset simulation. Using the above information it can be shown that the gradient of the failure probability function with respect to the design variable χ_l is given by (Jensen et al, 2009)

$$\left. \frac{\partial P_F(\{\chi\})}{\partial \chi_l} \right|_{\{\chi\}=\{\chi^k\}} \approx -\psi_1 \delta k_l P_F(\{\chi^k\}) \quad , \quad l = 1, \dots, n_d \quad (17)$$

where δk_l is the l -th element of the vector $\{\delta k\}$, and all other terms have been previously defined. This approach for estimating the gradients of the failure probability functions requires a single reliability analysis plus the evaluation of the demand function in the vicinity of the current design.

6 APPLICATION TO OFFSHORE STRUCTURES

6.1 Stochastic sea model

The random sea is modeled as a Gaussian process following a JONSWAP (Joint North Sea Wave Observation Project) type spectrum for the free surface elevation (Hasselmann and Olbers, 1973)

$$S(f) = \frac{\alpha g^2}{(2\pi)^4 f^5} \exp \left[-1.25 \left(\frac{f}{f_p} \right)^{-4} \right] \gamma^{\exp \left(-\frac{(f/f_p - 1)^2}{2\sigma^2} \right)} \quad (18)$$

where f is the frequency, α an equilibrium coefficient, σ a dimensionless spectral width parameter with value σ_a for $f < f_p$ and value σ_b for $f > f_p$, f_p the peak frequency, γ a peakedness parameter, and g the gravitational acceleration. For illustration, Figure (1) shows the spectrum corresponding to the values $\alpha = 0.015$, $\sigma_a = 0.07$, $\sigma_b = 0.09$, $f_p = 0.1$ Hz, and $\gamma = 3.3$.

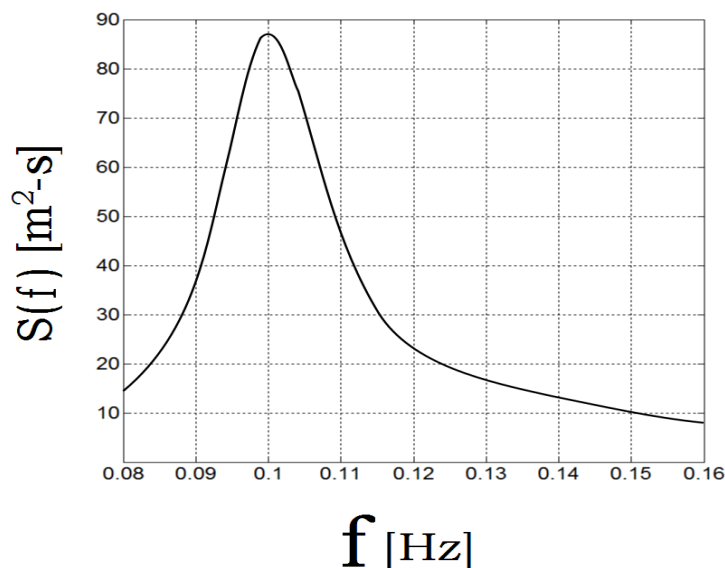


Figure 1: JONSWAP spectrum for the free surface elevation

To implement this spectrum the free surface wave elevation is represented in the time domain by a superposition of harmonic waves corresponding to different frequencies $\omega_i = 2\pi f_i, i = 1, \dots, M$

$$\eta(x, t) = \sum_{i=1}^M A_i \cos(k_i x - \omega_i t + \nu_i) \quad (19)$$

with

$$A_i = \sqrt{4S(f_i)\Delta\omega_i} \quad (20)$$

where x is the horizontal distance where the free surface elevation is evaluated, k_i is the wave number, ν_i is a uniform random variable defined in $[0, 2\pi]$, and $\Delta\omega_i = 2\pi\Delta f_i$ is the band width that each harmonic represents. For determining the sequence $\{\omega_i\}, i = 1, \dots, M$ the frequency range is divided into equal sub-ranges and ω_i is chosen as the middle of each one. The bandwidth $\Delta\omega_i$ equals the width of the respective sub-range. It is noted that the frequency ω_i and the wave number k_i are related according to the so-called dispersion relationship. A sample realization of the free surface elevation corresponding to the spectrum presented in Figure (1) is shown in Figure (2).

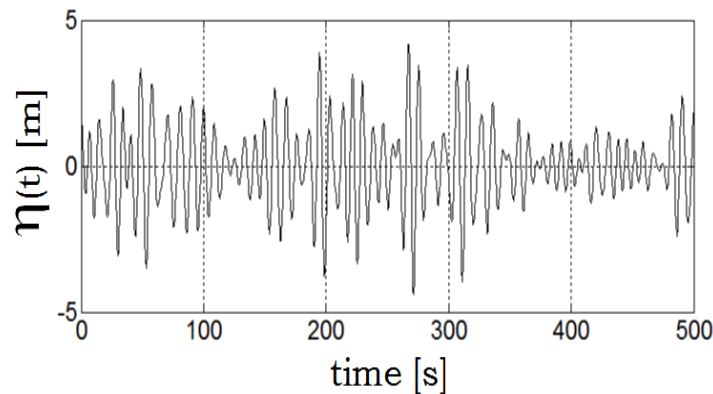


Figure 2: Sample realization of the free-surface elevation

The water particle kinematics are computed according to Airy linear wave theory (Hudspeth, 2006). The water particle velocity v and acceleration a in the horizontal direction are given respectively by

$$v(x, z, t) = \sum_{i=1}^M A_i \omega_i Z_i(z) \cos(k_i x - \omega_i t + \nu_i) \quad (21)$$

$$a(x, z, t) = \sum_{i=1}^M A_i \omega_i^2 Z_i(z) \sin(k_i x - \omega_i t + \nu_i) \quad (22)$$

with

$$Z_i(z) = \frac{\cosh(k_i z)}{\sinh(k_i (d + \eta(x, t)))} \quad (23)$$

where z is the water elevation measured from the ocean bottom.

6.2 Hydrodynamic forces

The hydrodynamic forces of the submerged portion of the structure are calculated using the Morison's modified wave force equation (Hudspeth, 2006). For a pile-type structure with diameter D the force in the normal direction, per unit of length, is given by

$$F(x, z, t) = \frac{1}{2}\rho_w DC_D [v(x, z, t) - \dot{y}(x, z, t)] [|v(x, z, t) - \dot{y}(x, z, t)|] + \frac{1}{4}\rho_w \pi D^2 C_M a(x, z, t) - \frac{1}{4}\rho_w \pi D^2 (C_M - 1) \ddot{y}(x, z, t) \quad (24)$$

where ρ_w is the density of the sea water, C_D is the drag coefficient, C_M is the inertia coefficient, $v(x, z, t)$ and $a(x, z, t)$ are as before the wave particle velocity and acceleration normal to the pile, and $\dot{y}(x, z, t)$ and $\ddot{y}(x, z, t)$ are the corresponding structural normal velocity and acceleration. The drag and inertia coefficients are assumed to be constant along the water depth and frequency independent. The last term of Equation (24) is referred to as the added-mass. For the evaluation of the hydrodynamic forces on the submerged portion of the structure the total length of the structural elements (piles) is divided into segments. The structural and wave kinematics are then calculated at the ends of each segment (nodal characterization). For the case of the wave kinematics, the corresponding nodal characterization is obtained as follows. First, the wave particle velocity and acceleration are multiplied by linear interpolation functions and then the product is integrated along each segment. These nodal forces are then incorporated into the equation of motion of the offshore structural model.

6.3 Equation of motion

The equation of motion of the offshore structural model is written as

$$[M_s]\{\ddot{y}_s(t)\} + [C_s]\{\dot{y}_s(t)\} + [K_s]\{y_s(t)\} = \{f_s(\{\dot{y}_s(t)\})\} \quad (25)$$

where $\{y_s(t)\}$ denotes the vector of nodal displacements of dimension n , $\{\dot{y}_s(t)\}$ the velocity vector, $\{\ddot{y}_s(t)\}$ the acceleration vector, and $\{f_s(\{\dot{y}_s(t)\})\}$ the vector of hydrodynamic forces. The matrices $[M_s]$, $[C_s]$, and $[K_s]$, describe the mass, damping and stiffness of the structural model, respectively. All these matrices are assumed to be constant with respect to time. Note that the excitation vector $\{f_s\}$ can be defined directly in terms of the free surface elevation $\eta(x, t)$, the wave particle velocity $v(x, z, t)$, the wave particle acceleration $a(x, z, t)$, and the velocity response vector $\{\dot{y}_s(t)\}$. The linearity of the structural model as well as the linearity of the wave theory for modeling the wave kinematics and estimating the hydrodynamic forces are assumptions for this particular study. The methodology discussed here, though, is appropriate for more complex cases, for example the consideration of nonlinear structural models and applications that consider nonlinear theories for modeling the wave kinematics. The numerical integration of the equation of motion is carried out by an appropriate step-by-step integration scheme.

7 NUMERICAL EXAMPLE

7.1 Description

An offshore structural model represented by a pile in a wave field, as schematically sketched in Figure (3), is considered for study. A mass of 2500 ton is supported by the circular column of diameter d . The nominal properties of the reinforced concrete pile element, which is fixed at the bottom, are given by: modulus of elasticity $E = 2.3 \times 10^{10}$ N/m²; and mass density $\rho = 2500$ kg/m³. The mean water depth is $h = 70$ m and the height of the pile is equal to $l = 75$ m. The wave field is modeled as a Gaussian process following a JONSWAP type spectrum for the free surface elevation with model parameters $\alpha = 0.015$, $\sigma_a = 0.07$, $\sigma_b = 0.09$, $f_p = 0.1$ Hz, and $\gamma = 3.3$. The drag and inertia coefficients are taken as $C_D = 1.5$ and $C_M = 2.0$, and the density of the sea water is equal to $\rho_w = 1.0 \times 10^3$ kg/m³. The Young's modulus E and the damping ratio of the model are treated as uncertain system parameters. The Young's modulus is modeled by a Log-normal random variable with most probable value $\bar{E} = 2.3 \times 10^{10}$ N/m², and coefficient of variation of 10%, while the damping ratio is modeled by a Log-normal random variable with mean value $\bar{\zeta} = 0.05$ and coefficient of variation of 40%. On the other hand, the total diameter D of the pile is also treated as uncertain due to the biofouling phenomenon. It is defined as $D = d + 2d_f$ where d_f is modeled by a Log-normal random variable with most probable value $\bar{d}_f = 0.1$ m, and coefficient of variation of 40%

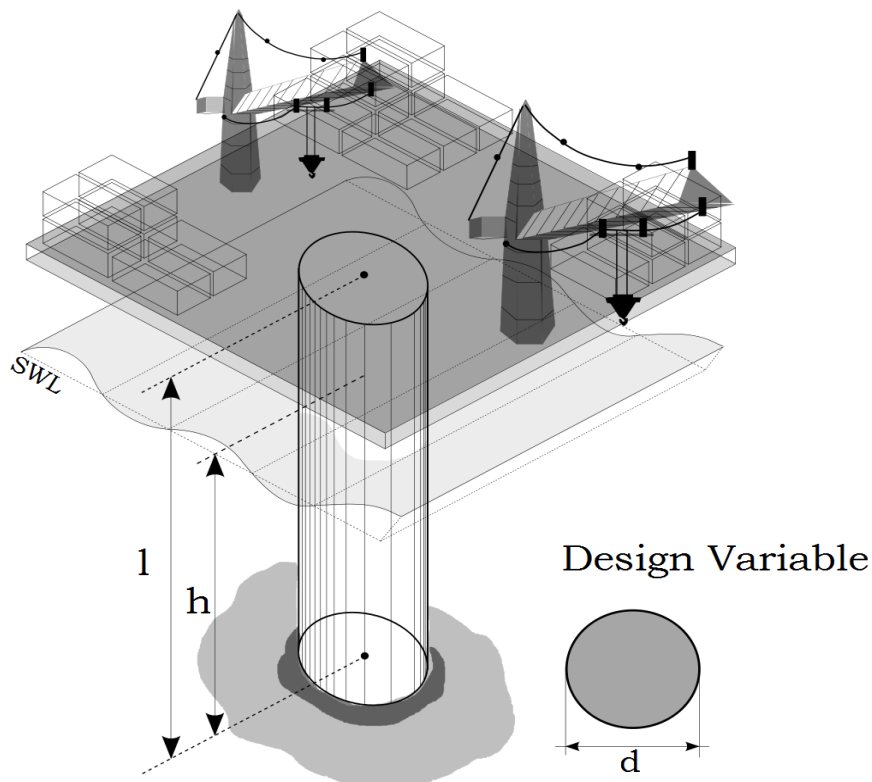


Figure 3: Offshore structural model

7.2 Design Problem

The analysis and design of the system is carried out in terms of the diameter d of the pile. The objective functions are expressed with respect to the initial cost (c_1), and the failure consequence cost (c_2). The initial or production cost is assumed to be proportional to the area of the cross section of the pile. On the other hand, the failure consequence cost is expressed in terms of the system failure probability $P_F(d)$ given a storm occurrence. The storm occurrences are modeled as a Poisson process with an occurrence rate of $\nu = 0.25$ per year. Then the probability of failure for a given reference or operation period ($T = 50$ years) is obtained by

$$P_{F|T}(d) = 1 - \exp[-\nu T P_F(d)] \quad (26)$$

Failure over the operation period is assumed to occur when the displacement at the deck (top of the pile) reaches some critical level for the first time. A threshold level equal to 0.75 m is considered. Thus, the failure event is defined as

$$F = \max_{t \in [0, t_s]} |y(t, d, \{\theta\})| > 0.75 \quad (27)$$

where $t_s = 8$ min is the time of analysis for a given storm, y is the displacement response at the top of the pile, and $\{\theta\}$ is the vector of uncertain parameters involved in the problem. The vector of objective functions to be minimized is $\{c_1(d), c_2(d)\}$ where the diameter d of the pile is constrained in the interval $[3.5, 5.0]$ m.

7.3 Results

The corresponding compromise programming problem to the previous design problem can be written as

$$\text{Min } z \quad (28)$$

subject to

$$\begin{aligned} c_1(d) &\leq z(c_1^{\text{as}} - c_1^{\text{id}}) + c_1^{\text{id}} \\ c_2(d) &\leq z(c_2^{\text{as}} - c_2^{\text{id}}) + c_2^{\text{id}} \\ 3.5 &\leq d \leq 5.0 \text{ m} \\ z &\geq 0 \end{aligned} \quad (29)$$

In the above equation c_1^{as} and c_2^{as} represent the aspiration level of the objective functions, while c_1^{id} and c_2^{id} are the corresponding ideal values (individual optima for each of the objective functions). The ideal point in the normalized objective function space $(c_1, c_2) = (9.62, 5.56)$ as well as the points corresponding to single objectives, i.e, initial cost minimization problem $(c_1, c_2) = (9.62, 7.99)$, and failure consequence minimization problem $(c_1, c_2) = (19.63, 5.56)$ are shown in Fig. (4). In this figure, the objective functions are normalized by appropriate factors. For illustration purposes the following aspiration level is considered: $(c_1, c_2) = (13.50, 7.00)$. By solving the compromise optimization problem the following design is obtained $(c_1, c_2) = (11.53, 6.26)$. For comparison, the Pareto front is also shown in the figure. It is seen that the point $(c_1, c_2) = (11.53, 6.26)$ is a Pareto point in the sense that no other solutions are superior to it when the two objective functions are considered simultaneously. It is also observed that the Pareto point minimizes the distance between the ideal point and the

Pareto front in the direction defined by the ideal point and the aspiration level. The trajectory of the optimization process corresponding to the compromise optimization problem in the design space is shown in Fig. (5). It is seen that the process converges in less than four iterations. Thus, the Pareto point is obtained in a very efficient manner. The same efficiency is found for other aspiration levels. Thus, the method is robust in terms of the aspiration levels considered in the analysis.

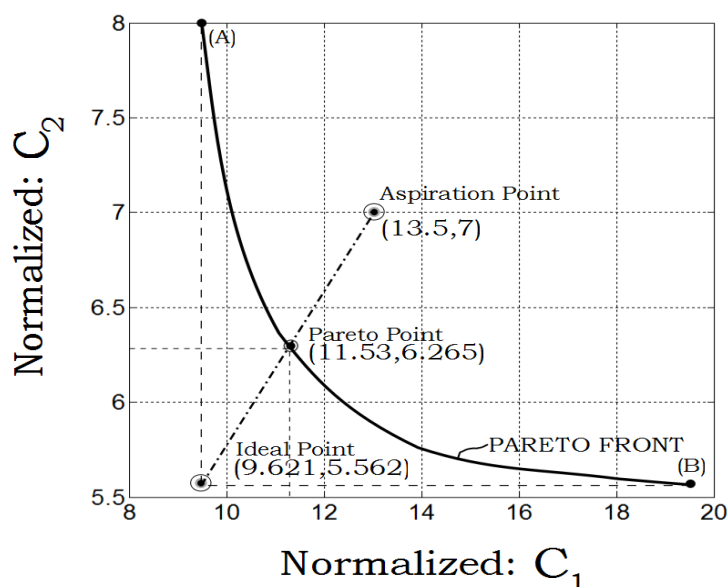


Figure 4: Pareto point in the normalized objective function space obtained by compromise optimization

As previously pointed out the sensitivity analysis at a given Pareto solution provides the information on the effect of changes in one objective function over the other objective along its feasible descent direction. In this case the feasible descent directions with the greatest improvement of the objective functions c_1 and c_2 are given by their steepest descent directions. The feasible direction of c_1 is negative while the feasible direction corresponding to c_2 is positive. This indicates for example that an increase in the diameter d will produce an increase in the initial cost and a decrease in the failure consequence cost. It is also found that an increase in the initial cost of the system is associated with a decrease in the failure consequence cost. Similarly, an increase in the failure consequence cost is achieved by a decrease in the initial cost. The fact that these sensitivities are negatives indicates that the current design is Pareto optimum.

8 CONCLUSIONS

The goal of the present work was to introduce an efficient computational procedure for multi-objective optimization of structural systems such as offshore structures under stochastic excitation. For that purpose several techniques such as compromise programming, advanced Monte Carlo strategies, and nonlinear interior point schemes have been integrated. Numerical results show that the total number of reliability analyses required during the entire design process is in general very small. Hence, different compromise solutions including the design that best represents the outcome that the designer considers potentially satisfactory are obtained in an efficient manner. At the same time an effective sensitivity analysis of Pareto solutions can be carried out by the proposed formulation. Such sensitivity information provides the designer

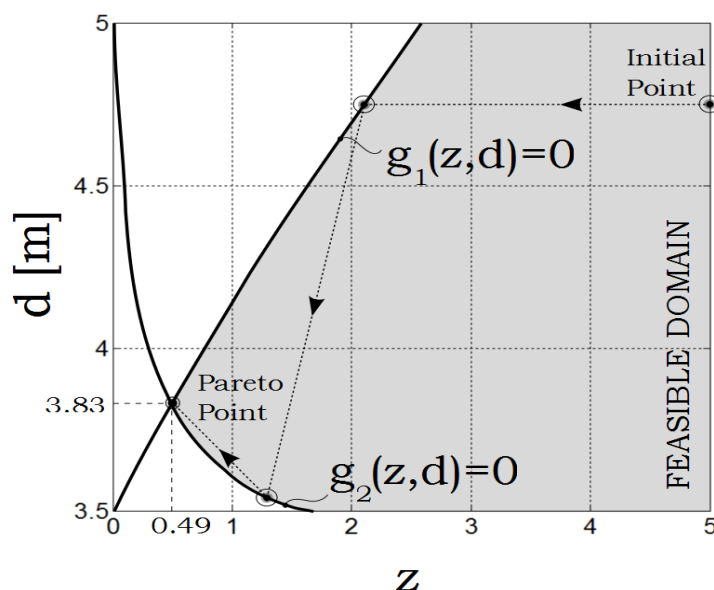


Figure 5: Trajectory of the optimizer for the compromise optimization problem in the design space

a practical tool for efficient exploration around Pareto solutions and for decision making and tradeoff analysis. It is concluded that the proposed multi-objective optimization procedure can be very effective in realistic engineering problems such as offshore structures under stochastic water wave excitation.

9 ACKNOWLEDGEMENTS

The research reported here was supported in part by CONICYT under grant number 1070903 which is gratefully acknowledged by the authors.

REFERENCES

- Au S.K. and Beck J.L., Estimation of small failure probabilities in high dimensions by subset simulation. *Probabilistic Engineering Mechanics*, 16(4):263–277, 2001.
- Belegundu A.D. and Chandrupatla T.R., *Optimization Concepts and Applications in Engineering*, Prentice Hall, New Jersey, 1999.
- Goldberg D.E., *Genetic Algorithms in Search, Optimization and Machine Learning*. Addison-Wesley, Reading, MA 1989.
- Haftka R.T. and Gürdal Z., *Elements of Structural Optimization*, Third edition, Kluwer Academic Publishers, The Netherlands. 1992.
- Hasselmann K. and Olbers D., 'Measurements of wind-wave growth and swell decay during the Joint North Sea Wave Project (JONSWAP)', *Hydrogr. Z., Reihe A* (8) 12, 1–95, 1973.
- Hudspeth R.T., *Waves and Wave Forces on Coastal and Ocean Structures*, Advanced Series on Ocean Engineering, Volume 21, World Scientific, 2006.
- Jensen H.A., Tradeoff Analysis of Non-Linear Dynamical Systems under Stochastic Excitation *Probabilistic Engineering Mechanics*, Vol. 24, 2009, pp. 585-599.

- Jensen H.A., Valdebenito M.A., Schuëller G.I., and Kusanovic D.S. Reliability-based optimization of stochastic systems using line search *Computer Methods in Applied Mechanics and Engineering*, 198(49-52), 2009, pp. 3915-3924
- Messac A. and Mattson C.A., Generating Well-Distributed Sets of Pareto Points for Engineering Design using Physical Programming. *Optimization and Engineering*, Vol. 3, 2002, pp. 431-450.
- Miettinen K.M, Nonlinear Multiobjective Optimization. *International Series in Operations Research and Management Science*, Kluwer Academic. Norwell, MA, 1999, pp. 29-43.
- Papadimitriou C., Pareto Optimal Sensor Locations for Structural Identification. *Computer Methods in Applied Mechanics and Engineering*, Vol. 194, 2005, pp. 1655-1673.
- Papadrakakis M., Lagaros N.D., and Plevris V., Multiobjective Optimization of Space Structures under Static and Seismic Loadings Conditions . *Engineering Optimization*, Vol. 34, 2002, pp. 645-669.
- Rao S.S., Venkayya V.B., and Khot N.S., Game Theory Approach for the Integrated Design of Structures and Controls. *AIAA*, Vol. 26(4), 1988, pp. 654-667.
- Sawaragi Y., Nakayama H., Tanino T., *Theory of Multiobjective Optimization*. Academic, Orlando, FL, 1985.
- Stadler W. and Daure J., Multicriteria Optimization in Engineering: A tutorial and Survey. *Structural Optimization: Status and Promise*, edited by M.P. Kamat, Vol. 150. Progress in Astronautics and Aeronautics, AIAA, Washington DC, 1992, pp. 209-244.
- Steuer R.E., *Multiple Criteria Optimization: Theory, Computation and Applications*, Wiley, New York, 1986.
- Tappeta R.V., Renaud J.E., Interactive Multiobjective Optimization Procedure. *AIAA Journal*. 1999. Vol. 37 (No 7) pp. 881-889.
- Ulrich K.T. and Eppinger S.D., *Product Design and Development*, 2nd Edition, McGraw-Hill, New York, 2000, pp. 138-159.
- Valdebenito M.A. and Schuëller G.I., Efficient strategies for reliability-based optimization involving non linear, dynamical structures. *IfM-Int. Work Report No.3-61*, Institute of Engineering Mechanics, University of Innsbruck, Austria. 2009.